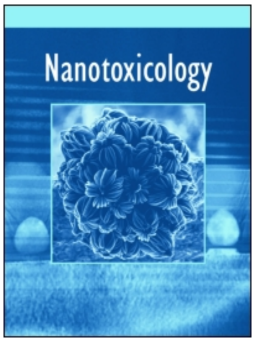

Taylor & Francis
Taylor & Francis Group

Nanotoxicology

ISSN: 1743-5390 (Print) 1743-5404 (Online) Journal homepage: http://www.tandfonline.com/loi/inan20

Silver nanoparticle toxicity is related to coating materials and disruption of sodium concentration regulation

Kevin W.H. Kwok, Wu Dong, Stella M. Marinakos, Jie Liu, Ashutosh Chilkoti, Mark R. Wiesner, Melissa Chernick & David E. Hinton

To cite this article: Kevin W.H. Kwok, Wu Dong, Stella M. Marinakos, Jie Liu, Ashutosh Chilkoti, Mark R. Wiesner, Melissa Chernick & David E. Hinton (2016): Silver nanoparticle toxicity is related to coating materials and disruption of sodium concentration regulation, Nanotoxicology, DOI: 10.1080/17435390.2016.1206150

To link to this article: http://dx.doi.org/10.1080/17435390.2016.1206150

Accepted author version posted online: 26 Jun 2016.
Published online: 26 Jun 2016.

Submit your article to this journal

Article views: 3

View related articles

View Crossmark data

Full Terms & Conditions of access and use can be found at
http://www.tandfonline.com/action/journalInformation?journalCode=inan20

Download by: [Duke University Libraries] **Date:** 30 June 2016, At: 13:10

Silver nanoparticle toxicity is related to coating materials and disruption of sodium concentration regulation

Kevin W.H. Kwok[1], Wu Dong[2,3], Stella M. Marinakos[4], Jie Liu[5], Ashutosh Chilkoti[6], Mark R. Wiesner[6], Melissa Chernick[2], David E. Hinton[2]*

1. Department of Applied Biology and Chemical Technology, The Hong Kong Polytechnic University, Hung Hom, Hong Kong SAR
2. Nicholas School of the Environment and Center for the Environmental Implications of Nanotechnology, Duke University; Durham, NC, USA
3. College of Animal Science and Technology, Inner Mongolia University for Nationalities, Tong Liao, China.
4. Department of Civil and Environmental Engineering and Center for the Environmental Implications of Nanotechnology, Duke University, Durham, NC, USA
5. Department of Biomedical Engineering and Center for the Environmental Implications of Nanotechnology, Duke University, Durham, NC, USA
6. Department of Chemistry and Center for the Environmental Implications of Nanotechnology, Duke University, Durham, NC, USA

Corresponding author: David E Hinton

Nicholas School of the Environment and Center for the Environmental Implications of Nanotechnology, Duke University; Durham, NC, USA

Tel: +1 919 613-8038; Email: dhinton@duke.edu

Downloaded by [Duke University Libraries] at 13:10 30 June 2016

JUST ACCEPTED

Downloaded by [Duke University Libraries] at 13:10 30 June 2016

ABSTRACT

Silver nanoparticles (AgNP) have been increasingly commercialized and their release into the environment is imminent. Toxicity of AgNP has been studied with a wide spectrum of organisms yet the mechanism of toxicity remains largely unknown. This study systematically compared toxicity of ten AgNPs of different particle diameters and coatings to Japanese medaka (*Oryzias latipes*) larvae to understand how characteristics of AgNP relate to toxicity. Dissolution of AgNPs was largely dependent on particle size but their aggregation behavior and toxicity were more dependent on coating materials. 96 h lethal concentration 50% (LC50) values correlated with AgNP aggregate size rather than size of individual nanoparticles. Of the AgNPs studied, the dissolved Ag concentration in the test suspensions did not account for all of the observed toxicity, indicating the role of NP-specific characteristics in resultant toxicity. Exposure to AgNP led to decrease of tissue sodium concentration and increased expression of Na^+/K^+ ATPase. Gene expression patterns also suggested that toxicity was related to disruption of sodium regulation and not by oxidative stress.

Keywords: oxidative stress, particle distribution, *Oryzias latipes*, coating, nanosilver

JUST ACCEPTED

Downloaded by [Duke University Libraries] at 13:10 30 June 2016

JUST ACCEPTED

INTRODUCTION

Nanoparticles are being introduced rapidly into the consumer market yet their potential impact on the environment and human health are not fully evaluated. Silver nanoparticles (AgNPs), in particular, with a current annual production that is estimated to be around 500 tons are widely used as commercial and medical products (Geranio et al. 2009; Silver Nanotechnology Working Group 2012; Reidy et al. 2013). The market for nanosilver materials and products is expected to grow substantially in value from US$290 million in 2011 to around US$1.2 billion by 2016 (Pistilla 2011).

Most AgNP-containing products are capitalizing on the antimicrobial property of silver (Seltenrich 2013). Accordingly, many products are personal hygiene related (*e.g.*, disinfecting sprays; Wijnhoven et al. 2009) within clothing, food utensils and medical products, contributing to >30% nano-containing products on an online consumer product inventory (www.nanotechproject.org).

Use and disposal of these products will inevitably result in release of AgNPs and their subsequent entry into aquatic environments. Release of AgNP from garments has already been demonstrated after as little as 5 washing cycles (Benn and Westerhoff 2008), underscoring the need for better understanding of AgNP toxicity to aquatic organisms. According to a recent risk assessment, ultimate fate of AgNP will be the aquatic environment (Nowack 2010). Using a sophisticated exposure model, predictions of resultant AgNP concentration in the aquatic environment are as high as 10 ug/L (Blaser et al. 2008). AgNP has already been detected in one municipal sewage system (Kim et al. 2010) and predicted concentrations for AgNPs in sewage sludge are 1.3-4.4 mg kg^{-1} (Gottschalk et al. 2009).

Downloaded by [Duke University Libraries] at 13:10 30 June 2016

Toxicity of AgNP had been demonstrated *in vitro* and *in vivo* in a wide range of aquatic species ranging from simple diatoms to invertebrates and vertebrates (*e.g.*, Bone et al. 2015; Kwok et al. 2012; Navarro et al. 2008; Yang et al. 2012). AgNP toxicity has been largely explained on the basis of Ag ions (Ag^+) (*e.g.*, Bone et al. 2015; Yang et al. 2012). In aquatic organisms, Ag^+ causes toxicity through disruption of sodium regulation. Experiments have shown that AgNP toxicity can be rescued when Ag ions are complexed by a thiol ligand (Yang et al. 2012) or cysteine (Navarro et al. 2008). However, other studies suggest AgNP toxicity to be attributable to reactive oxygen species (ROS) formed on the surface of AgNPs (Kim et al. 2009). Because the mechanism of AgNP toxicity remains in question, additional investigations are needed. AgNP toxicity is further complicated by the fact that coatings are commonly used to facilitate their stability and dispersion in aqueous media. Past toxicity studies have used differently coated AgNPs such as polyvinylpyrrolidone (Wu et al., 2011), metal oxide (Griffitt et al., 2009) or undefined coatings (Chae et al., 2009), making comparison difficult.

JUST ACCEPTED

Our previous study compared AgNPs and showed differential AgNP toxicity with different surface coatings (Kwok et al., 2012). However, these conclusions were partially confounded by the different particle sizes of the AgNPs. While other studies confirm that coatings of AgNP can affect toxicity in cells and invertebrates (Yang et al. 2012; Suresh et al. 2012; Zhao and Wang 2012) whether this effect extends to vertebrates is unknown. To better understand mechanisms of toxicity of AgNPs in aquatic environment and the effect of coatings, this study systematically compared toxicity of 10 different AgNPs with different coatings and sizes in an aquarium model fish, relating their toxicities with AgNP characteristics and properties in test media, and the underlying mechanism of toxicity.

MATERIALS AND METHODS

Synthesis and characterization of silver nanoparticles

A total of ten AgNPs of different coating and diameters were used in this study. Their particle diameter, zeta potential, dissolved fraction and abbreviations were presented in Table 1. Particle diameter was determined by measurement of diameters of 100 particles under transmission electron microscopy (TEM). Zeta potential of each AgNP dispersed in test medium for this study was measured after 24 and 96h by zetasizer (Malvern, UK). Aggregation size was measured based on hydrodynamic diameter of each AgNP dispersed in the test medium after 24 and 96h using zetasizer (Malvern, UK). Dissolved Ag concentration of 10 mg Ag L^{-1} AgNPs suspended in test medium was measured at 24 and 96h using ICP-MS (Agilent 7700x ICP-MS, Agilent Technologies, Santa Clara, CA, USA) by collecting the supernatant after centrifugation (197,568 × g for 1 h) and acidification with 2% HNO_3 in dark overnight at room temperature (Kwok et al. 2012). Dissolved fraction at 96h LC50 values was estimated based on dissolved Ag concentration of each AgNP at 10 mg Ag L^{-1}.

Except for citrate glutathione coated AgNPs (Cit-AgNPs), transmission electron micrograph and characterization data of the other AgNPs can be found from the references presented in Table 1. For Cit-AgNPs, the synthesis method was as follows: 100g $AgNO_3$ was dissolved in 80ml of Nanopure water and was heated to 60^{o}C. Then 20 mL solution containing 35mg trisodium citrate and 120 µg glutathione were added under vigorous stirring until the colorless

Downloaded by [Duke University Libraries] at 13:10 30 June 2016

JUST ACCEPTED

solution became yellow. At this time the solution was boiled for 20 min, resulting in nanoparticles ~25 nm in diameter (Fig. S 3).

Acute Exposure

Orange-red (OR) medaka (*Oryzias latipes*) were maintained at the Duke University Aquatic Research Facility under standard recirculating water conditions. Animal care and maintenance protocols, approved by the Duke University Institutional Animal Care and Use Committee were strictly followed. Medaka larvae (<8 hph) were collected and selected for normal developmental characteristics. Then they were individually placed in one of 12 wells in microplates, each containing 2 ml test suspension. The stock suspensions of the different of AgNPs were diluted in United States Environmental Protection Agency (USEPA) moderately hard water to reach desired test concentrations. This reconstituted freshwater contained 96 mg L^{-1} $NaHCO_3$, 60mg L^{-1} $CaSO_4 \cdot 2H_2O$, 60mg L^{-1} $MgSO_4$ and 4.0mg L^{-1} KCl. To establish the 96h lethal concentration for 50% of the test individuals (LC50), a total of 36 hatchlings (12 × 3 replicates) were exposed to each treatment and test concentration. Fish were exposed to 7-8 concentrations of each AgNP (0, 0.1, 0.2, 0.5, 1, 5, 10, 15 mg Ag L^{-1}). In addition, fish were exposed to 30-250 µg Ag L^{-1} $AgNO_3$ (corresponding to the dissolved Ag fraction of the highest test concentration of each AgNP). For all experiments fish were maintained at 25±0.5ºC, pH 7.5-7.7, hardness 82-85 mg L^{-1}, and a 14:10 light:dark cycle in EPA water. Recently, test medium composition and silver speciation in medium influencing toxicity (*e.g.*, Groh et al. 2014, Yue et al. 2014) were reported. Both investigations concluded that ionic strength and chloride ion concentration in medium heavily influenced AgNP toxicity. Therefore in this study, comparison of AgNP toxicity was

Downloaded by [Duke University Libraries] at 13:10 30 June 2016

JUST ACCEPTED

determined in a single, identical medium of low chloride ion concentration to eliminate possible effects from test medium.

Whole body silver and sodium measurement

Medaka larvae (<8 hph) were exposed to the 96h LC50 of each AgNP for 48h. Triplicates of 6 pooled fish per treatment were weighed to the nearest 0.1mg, rinsed 3 times in MilliQ water and digested in 2 ml concentrated HNO_3 at 90°C overnight. The digested samples were then diluted 20 fold in 0.5% HCl and 2% HNO_3 and whole body Ag and sodium (Na) concentrations were measured using ICP-MS (Agilent 7700x ICP-MS, Agilent Technologies, Santa Clara, CA, USA). Dogfish muscle (DORM-2, National Research Council Canada) was used as reference material for both Ag and Na measurements. Measurement recovery of Ag and Na were 88.9% and 90.4% respectively.

Real Time-PCR

Four replicates of 10 fish (<8hph) were exposed to the 96h LC50 concentration of each AgNP for 48h. Then, fish were euthanized and total RNA was extracted using a commercial kit according to manufacturer's instruction (Qiagen RNeasy Mini Kit, USA) and immediately reverse transcribed into cDNA using reverse transcriptase (SuperScript® II Reverse Transcriptase, Invitrogen, USA). Four oxidative biomarker genes, metallothionine (MT), superoxide dismutase (SOD), glutathione sulfur transferase (GST) and Cytochrome P450 (CYP1a) were expressed. In addition, Na^+/K^+ ATP1a1 (NKA), an important gene for sodium regulation in fish, was quantified using SYBR green (SYBR® Green PCR Master Mix, Applied Biosystems, USA). Expression of all genes was normalized against 18S RNA gene and fold

Downloaded by [Duke University Libraries] at 13:10 30 June 2016
JUST ACCEPTED

Downloaded by [Duke University Libraries] at 13:10 30 June 2016

change was calculated using methodology described in Rao et al. (2013). Primers used are summarized in Table 2.

Paraffin section enhanced dark field hyperspectral imaging

Biodistribution of AgNPs was investigated using the exact method described in Kwok et al. (2012). In brief, three medaka that survived the highest concentration of each individual AgNP for 96h were anesthetized then fixed in 4% paraformaldehyde in 0.1M phosphate buffered saline (PBS). Upon embedment in paraffin, individuals were serially sectioned at 6 μm thickness. Alternate ribbons of sections were cleared and coverslipped without staining for examination using the enhanced dark field hyperspectral imaging (Cytoviva, USA) to locate AgNPs. To create a spectral library for each AgNP, a reference sample of each NP was dispersed in the test medium, applied to a clean glass slide and allowed to air-dry, and scanned by hyperspectral imaging. Next, unstained sections of control/exposed fish were examined for signals of NPs in tissues. Computerized identification of the characteristic hyperspectral signal of the target AgNP in fish sections was based on an angular displacement function with a significance threshold of 0.05. For both hyperspectral and light microscopic analyses, 5-6 parasagittal sections per fish, 20-25 μm apart (*i.e.*, non-overlapping) were examined with emphasis on the major organs (*i.e.*, brain, eye, gill, heart, kidney, liver, skeletal muscle and epidermis).

JUST ACCEPTED

Whole mount in situ hybridization and immunohistochemistry double staining

Measuring the gene expression pattern using whole organisms may not be ideal since expression patterns of many non-target cells may overwhelm the responses from fewer responding cells (Dong et al. 2013). In addition, the location of responses provides important

Downloaded by [Duke University Libraries] at 13:10 30 June 2016

information to correlate with sites of uptake as shown in hyperspectral images. Therefore whole mount *in sit*u hybridization and immunohistochemistry double staining procedures were used to better understand how NKA expression was changed by AgNP exposure. Larval fish were exposed to 96h LC50 for 48h and euthanized, then they were fixed in 4% paraformaldehyde in 0.1M PBS, slowly transferred to 100% methanol then stored at -20°C until processing. The samples were first transferred back into 1xPBS in a stepwise manner, followed by treatment with 10μg L^{-1} proteinase K in PBS with 0.1% Tween 20 (PBST). Whole mount *in situ* hybridization was then carried out according to (Dong et al. 2002). Embryos were hybridized with an antisense probe of 722 base pairs for medaka ATPα1a (Thermes et al. 2010). To generate the DIG-labeled RNA probe, a template DNA was synthesized with the forward primer, 5′-AGGAGGAGCCAGCAAACGATAAT-3′; reverse primer, 5′-TTCCAGGTTCTTCACCAAGCAAT-3′. Next, the DNA was inserted into pGEM vector (Promega, WI, USA) and transfected by sp6 RNA polymerase (Roche Mannheim, Germany). Following hybridization overnight at 64 °C, embryos were washed with 2 × SSC (300 mM NaCl, 30 mM sodium citrate, pH 7.0) and 0.2 × SSC twice for 30 min, respectively. Next the samples were blocked with 2% blocking reagent (Roche, Mannheim, Germany) and then incubated overnight with 3000 × diluted anti-DIG antibody conjugated with alkaline phosphatase (Roche) at 4 °C. Lastly, the color reaction was carried out by incubation with BM-purple substrate (Roche). The *in situ* hybridization samples were then subjected to immunohistochemistry to label the NKA protein. After washing with PBS, samples were incubated with 3% bovine serum albumin and 5% goat serum for 30min to block nonspecific binding. Samples were then incubated overnight at 4°C with α5-monoclonal antibody (chicken Na, K-ATPase 1:100 diluted) against the α-subunit of the avian Na^+ pump (Developmental Studies Hybridoma Bank,

JUST ACCEPTED

University of Iowa, Ames, IA). This antibody can specifically label NKA protein expressing cells in medaka larvae (Wu et al. 2010). After rinsing with PBS for 20 min, samples were further incubated in anti-mouse IgG antibody (1:200 dilution) for 2h at room temperature. Finally samples were washed twice with PBST for 20min each and stored in PBS at 4 °C in a dark box until imaging. For each fish, the right lateral abdominal surface was selected as a region of interest and the surface area was measured using NIH ImageJ 1.48 (Rasband, 2015) and the number of NKA gene/protein positive cells in this area was counted. Number of NKA positive cells per area were calculated for each treatment and compared.

Statistical Analyses

96h LC50 values and their 95% confidence intervals (CI) were determined using non-linear regression (GraphPad Prism 6.0, GraphPad Software, USA). Other endpoints were analyzed using one-way ANOVA followed by Tukey's test (SPSS version 22.0, IBM, USA). Percentage data was arcsine-square root transformed before ANOVA. Correlations between endpoints also were tested using SPSS. A multiple linear regression (stepwise model) was fitted to determine which AgNP characteristic and toxicity endpoint provided the best prediction of 96h LC50 values using SPSS.

RESULTS

Aggregation and dissolution of AgNPs in test medium

The hydrodynamic diameters of all AgNPs in USEPA water were greater than their respective diameter as determined by transmission electron microscopy (TEM), indicating aggregation (Table 1). Aggregation behavior of AgNPs was strongly influenced by the coating material rather

Downloaded by [Duke University Libraries] at 13:10 30 June 2016

JUST ACCEPTED

Downloaded by [Duke University Libraries] at 13:10 30 June 2016

JUST ACCEPTED

than the size of individual NPs. For PVP-AgNPs, their hydrodynamic diameters were stable around 100nm throughout the 96h test period (Table 1). For gum arabic (GA)-AgNPs, hydrodynamic diameter and polydispersity index increased sharply from 24h to 96h, indicating that the NPs were unstable in USEPA water. For Cit-AgNPs, although aggregation size only increased slightly from 24h to 96h, the polydispersity index was the highest of the three coating materials groups (Table 1).

Dissolution of AgNP was mostly particle size dependent (Table 1). Significant correlation between dissolved Ag at 96h and particle size ($R = 0.723$, $p < 0.05$) was observed. Smaller AgNPs generally dissolved more rapidly. For example, 6nm GA AgNP had a dissolution of 1.65% while the value for 23nm GA AgNP was 0.30% after 24h.

Acute Toxicity

All AgNPs proved acutely toxic to medaka with 96h LC50 values ranging from 0.55-5.05 mg Ag L^{-1} (Fig. 1). The LC50 values did not correlate with their TEM diameter (R= 0.182, p>0.05). However, LC50 values of AgNPs were clustered by coating material (Fig. 1). GA-AgNPs were the most toxic, followed by PVP-AgNPs and Cit-AgNP type were the least toxic. Time to mortality for individual AgNP exposures also showed a similar effect of coating material. Exposure to GA-AgNP led to mortality in less than 36h, whereas for PVP-AgNP mortality occurred between 24-72h exposure. Cit-AgNP type caused mortality between 72-96h (data not shown). There was a significant correlation between aggregation size of AgNP at 24h and LC50 value (R= 0.685, p<0.01), but the relationship did not hold for aggregation size at 96h (R= 0.254, p>0.05).

Dissolved Ag concentration (μg Ag L^{-1}) in the test suspension was not correlated with LC50 values (R= 0.058, p>0.05) and was not a good predictor of AgNP toxicity. An interesting pattern was observed when LC50 values of each AgNP were expressed in terms of dissolved Ag present (Fig. 2). When compared with the LC50 value of AgNO3, Cit-AgNPs were consistently less toxic (*i.e.*, requiring a higher concentration of Cit-AgNPs to reach the LC50 of AgNO3). GA-AgNPs were consistently more toxic than $AgNO_3$ (Fig. 2). For PVP-AgNPs, a size dependent relationship was observed, with larger NPs more toxic than $AgNO_3$ and smaller NPs less toxic (Fig. 2).

Whole body silver and sodium concentration

Whole body Ag concentration, including AgNPs and silver in ionic and other forms, increased by 3-30 fold after 48h of exposure to AgNPs and $AgNO_3$ (Fig. 3). The $AgNO_3$ and 7nm Cit-AgNP (Cit7) exposed group has the highest whole body Ag concentration (μg/g wet weight), followed by other Cit-AgNPs and then GA- and PVP-AgNPs. Whole body Ag concentration was not related to AgNP particle size (R = 0.15, p>0.05). However, it was positively correlated to LC50 value, indicating that high Ag accumulation in fish tissue was related to low acute toxicity (Fig. 5a; R = 0.86, p<0.001).

Exposure to AgNP and $AgNO_3$ significantly reduced whole body Na concentration compared to controls (Fig. 4). $AgNO_3$and GA AgNPs showed similar magnitude of effect on whole body Na, decreasing whole body Na levels by about 30%. PVP and Cit-AgNPs had less of an impact on whole body Na, decreasing whole body Na levels by about 20% (Fig. 4). Significant

Downloaded by [Duke University Libraries] at 13:10 30 June 2016
JUST ACCEPTED

correlation was detected between whole body Na concentration and LC50 value (Fig. 5b; R = 0.78, p<0.01) but not between whole body Ag concentration and Na concentration (R = 0.30, p>0.05), indicating that body Ag concentration cannot explain the decrease in Na body concentration.

Biodistribution of AgNP

All AgNPs were detected in gills of all samples (Fig. 6a). Interestingly, all PVP-AgNPs and Cit7 were found in mid-brain region (Fig. 6b) but no other AgNPs were not found at this site. PVP-AgNPs were only found in the liver of two of the fish examined (data not shown). No AgNPs were detected in the epidermis, gut, or trunk kidney of any fish (data not shown). These findings were similar to that reported by Kwok et al. (2012).

Biomarker gene expression

CYP1a expression was significantly up-regulated by all AgNPs exposures but not by $AgNO_3$ (Fig 7a). Oxidative stress genes were not impacted by AgNP exposure. GST expression was significantly up-regulated by $AgNO_3$ and PVP 55k AgNP only, while SOD was significantly up-regulated by $AgNO_3$, PVP55k and large GA AgNP only. MT expression was only significantly up-regulated by $AgNO_3$ (Fig. 7). On the other hand, NKA was significantly up-regulated by $AgNO_3$ and all AgNPs except Cit7 and Cit-Tannic acid AgNPs of 24nm (Cit-TA24) (Fig. 7). Increase in NKA expression level was found to correlate to the decrease of whole body Na concentration (R=0.619, p<0.05) and LC50 values (*i.e.*, NKA expression increased as toxicity increased; R=0.632, p<0.05).

Downloaded by [Duke University Libraries] at 13:10 30 June 2016

JUST ACCEPTED

Downloaded by [Duke University Libraries] at 13:10 30 June 2016

Localization of Na^+/K^+ ATPase expression and translation

Both NKA gene- and protein- positive cells were co-localized on the lateral abdominal wall overlying yolk surface, pharyngeal endoderm and gill arches (Fig. 8a). Location of NKA gene and protein expression matched with previous reports (Thermes et al. 2010, Wu et al. 2010). All treatments except Cit-TA24 led to significant increase in number of NKA expressing cells relative to control as indicated by Dunnett's test following one-way ANOVA (Fig. 8b). The number of cells expressing NKA gene was increased to the greatest extent by GA-AgNP at 26nm (GA26), followed by GA5 and PVP-AgNPs, then $AgNO_3$and Cit-AgNPs. Number of NKA protein positive cells was increased most by PVP38, followed by GA5.

Particle characteristic and toxicity endpoints that predict AgNP LC50 values

A multiple linear regression (stepwise model) was fitted to determine which AgNP characteristics and toxicity endpoints provided the best prediction of 96h LC50 values. A combination of two factors, namely polydispersity index at 24h and whole body Na concentration, provided the best prediction of 96h LC50 values of AgNPs. The model had an adjusted R^2 of 0.854 and can be summarized by the following equation:

96h LC50 = 6.353*polydispersity index24h + 0.018*whole body Na concentration – 15.806

All other AgNP characteristics and toxicity endpoints were not significant in the model.

JUST ACCEPTED

DISCUSSION

AgNP behavior upon dissolution in test medium

Downloaded by [Duke University Libraries] at 13:10 30 June 2016

All AgNPs had low solubility in USEPA water. After 96h, the dissolved fraction in the test suspension ranged from 0.25% to 1.99%. Concentration of the dissolved fraction was comparable to earlier studies using the same medium and a subset of the AgNPs tested in this study (Kwok et al. 2012; Yang et al. 2012). In general, dissolved Ag fraction was higher for smaller diameter AgNPs. This finding is similar to Ma et al. (2012) who reported solubility of AgNP (5-40nm) where AgNP solubility was considered to be influenced by particle diameter rather than coating or synthesis methods.

Unlike dissolution, aggregation behavior was largely related to coating and not to particle diameter. PVP-AgNPs proved the most stable in USEPA water with the lowest polydispersity index among the three coating groups and a stable aggregation size from 24h to 96h. For GA-AgNPs, they were highly dispersed at 24h but their hydrodynamic diameter and polydispersity index increased sharply from 24h to 96h. The latter could indicate that they were unstable in USEPA water. Cit-AgNPs had high polydispersity index despite having a relatively average stable aggregation size (Table 1), possibly indicative of a small number of large aggregates in the test suspension.

JUST ACCEPTED

Characteristics of AgNP and its toxicity

Toxicity of AgNPs to medaka larvae (96h LC50: 0.55 – 5.05 mg L^{-1}) was in good agreement with reports based on other species or even cell lines. Laban et al. (2010) reported LC50 of fathead minnow embryos at 9.4 – 10.6 mg L^{-1} AgNP dispersed by stirring and at 1.25 – 1.36 mg L^{-1} for those dispersed by sonication. In the nematode *Caenorhabditis elegans*, Yang et al. (2012) reported an EC50 of population growth at 8 to 369 μM (0.86 – 39.8 mg L^{-1}) and Ahn et al. (2014) reported 24h LC50 of PVP-AgNPs between 0.6 to 3.2 mg L^{-1}. *In vitro*, cell culture studies showed AgNP toxicity in a similar concentration range. For example, significantly decreased viability of human bronchial epithelial cells to 50% of their pre-exposure numbers resulted from exposure to 10nm AgNPs between 20-50 uM (2.16 – 5.39 mg L^{-1}) (Gilga et al. 2014).

Size dependent toxicity of AgNPs has been reported *in vitro* (*e.g.*, Gilga et al. 2014; Kim et al. 2012; Park et al. 2011) and some *in vivo* tests (*e.g.*, Asghari et al. 2014; Gorth et al. 2011). These studies compared AgNPs with large difference in diameters (*e.g.*, 20-30nm, 100nm and >500nm in Gorth et al. 2014; 10nm, 40nm and 75nm in Gilga et al. 2014). However, when comparing particles with the smaller difference in diameters (20nm, 40nm, 60nm, 80nm and 100nm), size dependent toxicity was not observed (Ivask et al. 2014). By comparing toxicity of 10 relatively small AgNPs (diameters of 6-49nm), the present study found toxicity to be correlated with aggregation size of AgNP in test medium rather than with their particle diameters. Dispersion dependent toxicity of AgNP was reported for zebrafish embryos (Kim et al. 2013). Therefore, for AgNPs in a narrower but better defined size range, their behavior in test medium could be more important than particle size. Such findings highlight the importance of understanding NP behavior in future nanotoxicity studies.

Interestingly, dissolved Ag concentration in AgNP test suspensions did not relate to toxicity. By expressing LC50 values of AgNPs in the amount of dissolved Ag present (Fig. 2), it was evident that NP specific toxicity was present for GA-AgNPs and the two larger PVP-AgNPs because much of the resultant toxicity could not be fully explained by the amount of dissolved

Downloaded by [Duke University Libraries] at 13:10 30 June 2016
JUST ACCEPTED

Downloaded by [Duke University Libraries] at 13:10 30 June 2016

Ag present. Bioavailability of dissolved Ag is also important to AgNP toxicity. Complexation of dissolved Ag with Cl^- ions in the test medium lowered toxicity (Navarro et al. 2015). Although the toxicity tests were carried out in the same medium with low Cl^- concentration and were assumed to impact bioavailability of dissolved Ag equally, the exact nature of this interaction between dissolved Ag and coating materials needs further study. The resultant change in dissolved Ag bioavailability is therefore another direction for further studies. By contrast, for Cit-AgNPs and the two smaller PVP AgNPs, toxicity was explained by the amount of dissolved Ag present. Cit-AgNPs may have offered some protection from dissolved Ag toxicity to medaka and this might result from the higher affinity of citrate for free Ag^+ in water (Yang et al. 2012), possibly lowering their concentration and the resultant toxicity.

JUST ACCEPTED

Acute toxicity of AgNPs was heavily influenced by coating material (Fig. 1) and the effect was consistent over the size range of AgNP tested (6-49nm). Aggregation size of AgNP in the test medium was also influenced by coating material (Table 1), making it difficult in this study to tease apart whether AgNP toxicity was truly related to aggregation size or to coating. The 96h LC50 values of AgNPs clustered according to surface coating. For example, GA-AgNPs were about two times more toxic than PVP-AgNPs and twenty times more toxic than Cit-AgNPs. In a similar study, toxicity of different AgNPs to *C. elegans* was also found to be influenced by coating material and, to a lesser degree, by particle size (Yang et al., 2012). Moreover, toxicity of AgNPs with different coating materials followed the same order observed in our study: GA > PVP > Cit AgNP (Yang et al. 2012). Coating materials and surface charge-dependent AgNP cytotoxicity was also observed by Suresh et al. (2012). Similar findings have been reported in toxicity of gold nanoparticles as well (Truong et al. 2013), suggesting that this coating effect might apply to other metallic NPs. Since most interaction of a nanoparticle with the surrounding environment occurs at its surface, coating materials have the potential to alter and influence these interactions, thereby influencing toxicity. Precise mechanism of how coating materials can impact toxicity remains unknown but warrants further investigation.

Possible Mechanism of AgNP Toxicity

Two mechanisms have been used to explain AgNP toxicity: 1) oxidative stress and/or 2) release of toxic Ag^+. AgNPs were known to release ROS as they dissolve in aqueous medium (He et al. 2012). In cells, AgNP toxicity is related to uptake, production of ROS and triggering antioxidant defense (see review by McShan et al. 2014). For aquatic organisms, oxidative damage caused by AgNPs has also been widely reported (*e.g.*, Chae et al. 2009; van Aerle et al. 2013; Wu and Zhou 2013). Chronic exposure to Cit-AgNPs significantly reduces GST and SOD activity in common carp (*Cyprinus carpio*) (Lee et al. 2012). Zebrafish embryos exposed to $0.03^{-1}.55$ ppm AgNP and Ag^+ showed depleted glutathione levels but normal antioxidant enzyme activities (Massarsky et al 2013). Of the four oxidative stress related genes measured, only CYP1a showed overall response to AgNPs in this study (Fig. 7). The other three genes (SOD, GST and MT) only responded to $AgNO_3$ and one to two types of AgNPs. It was interesting that PVP-AgNP at 8nm but no other PVP-AgNPs caused up-regulation of two oxidative stress gene markers (SOD and MT). However, the lack of response of oxidative stress marker genes as a whole did not support oxidative stress as an important mechanism of AgNP toxicity to larval medaka.

Downloaded by [Duke University Libraries] at 13:10 30 June 2016

JUST ACCEPTED

The second proposed mechanism of AgNP toxicity relates to the release of Ag^+. Ionic Ag is well-known to cause toxicity through disruption of Na regulation (Bianchini et al. 2002; Wood et al. 1996; Wood 2011) and studies have shown that NKA is one of the primary targets of ionic Ag toxicity (Grossel et al. 2002). NKA is a universal membrane-bound enzyme that actively transports Na^+ out of and K^+ into animal cells. It is important not only for sustaining intracellular homeostasis but also for providing a driving force for many transporting systems in a variety of osmoregulatory epithelia including fish gills (McCormick 1995), which absorb ions and maintain acid-base balance in freshwater fish (Wood and Marshall 1994). In our study, whole body Na concentration of fish was decreased significantly by AgNP exposure. Recently, Schultz et al. (2012) also reported that AgNP inhibited Na uptake in juvenile rainbow trout (*Oncorhyncus mykiss*) through inhibition of NKA activity. This can potentially explain why whole body Na concentration decreased after AgNP exposure and how AgNP toxicity was related to disruption of Na regulation. Increased expression of NKA gene and protein after AgNP exposure implies the host is mounting a compensatory response. Disruption of NKA, reported in zebrafish and marine medaka (*Oryzias melastigma*) after AgNP exposure (Griffitt et al. 2009; Wang and Wang 2013) reflect the need for the above response. Overall, our data indicated that AgNP likely shared the same toxic mechanism as Ag^+ to larval medaka.

Our observed AgNP toxic mechanism may be explained by localized release of Ag^+ from AgNPs on the fish's body surface and causing toxicity. The membrane-spanning enzyme NKA is located in the ionocytes of the skin and mitochondria-rich cells in the gills (Hwang and Lee 2007). These cells secrete acids (H^+ or NH_4^+) that regulate transepithelial absorption of Na^+ (Hwang and Lee 2007). Therefore a local pH difference surrounding these cells might be

Downloaded by [Duke University Libraries] at 13:10 30 June 2016

JUST ACCEPTED

expected. Higher release of Ag^+ from AgNPs occurs at lower pH than neutral pH (Peretyazhko et al. 2014). Thus, one can expect local pH around the cells where NKA is expressed to be more acidic and thereby to release Ag^+ from AgNPs, which could create “hotspots” of exposure that coincide with the immediate surroundings of the cells targeted in NKA toxicity.

Interestingly, AgNP was detected not only in the gill, but also in liver and brain. The presence of AgNP in deep tissues but not in all surficial tissue indicated presence of certain mechanism of biodistribution. This is similar to the report from Böhme et al. (2015) where total Ag tissue distribution changed through time in zebrafish embryos and the tissue Ag concentration related positively with toxicity. Conversely, we found that AgNP toxicity had no relationship to dissolved Ag concentration in test media, being negatively correlated to tissue Ag concentration (*i.e.*, toxicity decreased when tissue concentration increased). This contrast reveals the difficulty of generalizing AgNP toxic mechanisms over different species and life stages.

Downloaded by [Duke University Libraries] at 13:10 30 June 2016

JUST ACCEPTED

Downloaded by [Duke University Libraries] at 13:10 30 June 2016

JUST ACCEPTED

CONCLUSION

By comparing the toxicity of 10 AgNPs of different diameters and coating materials, we found that toxicity of AgNPs was independent of particle size but related to size of aggregates in test medium. Furthermore, toxicity of aggregates was heavily influenced by the coating material. Interestingly, AgNP exposure did not cause a significant response in three out of four oxidative marker genes examined. Rather, AgNP appeared to cause toxicity and with a similar toxic mechanism of Ag ions, disruption of Na regulation. Up-regulation of NKA was observed after exposure to AgNP and led to a decrease of whole body Na levels. Toxicity of AgNP did not correlate with dissolved Ag concentration in the test medium and may instead be related to localized release of Ag^+ on the surface of fish. More detailed studies examining AgNP related alterations to mitochondria rich cells and osmoregulatory surfaces of individual larvae under high resolution are needed to more conclusively elucidate the exact mechanisms of toxicity.

DECLARATION OF INTEREST

The authors report no conflict of interest. This paper is based upon work supported by the National Science Foundation (NSF) and the Environmental Protection Agency (EPA) under NSF Cooperative Agreement EF-0830093, Center for the Environmental Implications of NanoTechnology (CEINT). Any opinions, findings, conclusions or recommendations expressed in this material are those of the author(s) and do not necessarily reflect the views of the NSF or the EPA. This work has not been subjected to USEPA for review and no official endorsement should be inferred.

Downloaded by [Duke University Libraries] at 13:10 30 June 2016

JUST ACCEPTED

REFERENCES

Ahn J-M, Eom H-J, Yang X, Meyer JN, Choi J. 2014. Comparative toxicity of silver nanoparticles on oxidative stress and DNA damage in the nematode, *Caenorhabditis elegans*. Chemosphere 108:343-352.

Asghari S, Johari SA, Lee JH, Kim YS, Jeon YB, Choi HJ, Moon MC, Yu IJ. 2012. Toxicity of various silver nanoparticles compared to silver ions in *Daphnia magna*. J Nanotech 10:14.

Benn TM, Westerhoff P. 2008. Nanoparticle silver released into water from commercially available sock fabrics. Environ Sci Technol 42:4133-4139.

Bianchini A, Grosell M, Gregory SM, Wood CM. 2002. Acute silver toxicity in aquatic animals is a function of sodium uptake rate. Environ Sci Technol 36:1763^{-1}766.

Blaser SA, Scheringer M, MacLeod M, Hungerbühler K. 2008. Estimation of cumulative aquatic exposure and risk due to silver: Contribution of nano-functionalized plastics and textiles. Sci. Total Environ 390:396–409.

Bone AJ, Matson CW, Colman BP, Yang X, Meyer JN, Di Giulio RT. 2015. Silver nanoparticle toxicity to Atlantic killifish (*Fundulus heteroclitus*) and *Caenorhabditis elegans*: a comparison of mesocosm, microcosm, and conventional laboratory studies. Environ Toxicol Chem 34:275-282.

Böhme S, Stärk HJ, Reemtsma T, Kühnel D. 2015. Effect propagation after silver nanoparticle exposure in zebrafish (Danio rerio) embryos: a correlation to internal concentration and distribution patterns. Environmental Science: Nano 2:603-614.

Colman BP, Espinasse BP, Richardson CJ, Matson CW, Lowry G, Hunt D, Wiesner MR, Bernhardt ES. 2014. Emerging contaminant or an old toxin in disguise? Silver nanoparticle impact on ecosystems. Envrion Sci Technol 48:5229-5236.

Chae YJ, Pham CH, Lee J, Bae E, Yi J, Gu MB. 2009. Evaluation of the toxic impact of silver nanoparticles on Japanese medaka (*Oryzias latipes*). Aquat Toxicol 94:320-327.

Dadosh T. 2009. Synthesis of uniform silver nanoparticles with a controllable size. Materials Lett 63:2236-2238.

Dong W, Macaulay L, Kwok KWH, Hinton DE, Stapleton HM. 2013. Using whole mount in situ hybridization to examine thyroid hormone deiodinase (DI) expression in embryonic and larval zebrafish: a tool for examining OH-BDE toxicity to early life stages. Aquat Toxicol 132-133:190-199.

Dong W, Teraoka H, Yamazaki K, Tsukiyama S, Imani S, Imagawa T, Stegeman JJ, Peterson RE, Hiraga T. 2002. 2,3,7,8-tetrachlorodibenzo-p-dioxin toxicity in the zebrafish embryo: local circulation failure in the dorsal midbrain is associated with increased apoptosis Toxicol Sci 69:191–201.

Geranio, L, Heuberger M, Nowack B. 2009. The Behavior of Silver Nanotextiles during Washing. Environl Sci Technol 43:8113-8118.

Gilga AR, Skoglund S, Wallinder IO, Fadeel B, Karlsson HL. 2014. Size-dependent cytotoxicity of silver nanoparticles in human lung cells: the role of cellular uptake, agglomeration and Ag release. Particles Fibre Toxicol 11:11.

Gorth DJ, Rand DM, Webster TJ. 2011. Silver nanoparticle toxicity in Drosophila: size does matter. Int J Nanomedicine 6:343-350.

Downloaded by [Duke University Libraries] at 13:10 30 June 2016

JUST ACCEPTED

Gondikas AP, Morris A, Reinsch BC, Marinakos SM, Lowry GV, Hsu-Kim H. 2012. Cysteine-Induced Modifications of Zero-valent Silver Nanomaterials: Implications for Particle Surface Chemistry, Aggregation, Dissolution, and Silver Speciation. Environ Sci Technol 46:7037–7045.

Gottschalk F, Sonderer T, Scholz RW, Nowack B. 2009. Modeled environmental concentrations of engineered nanomaterials (TiO_2, ZnO, Ag, CNT, Fullerenes) for different regions. Environ Sci Technol 43:9216–9222

Griffitt, R.J.; Hyndman, K.; Denslow, N.D.; Barber, D.S. 2009. Comparison of molecular and histological changes in zebrafish gills exposed to metallic nanoparticlles. Toxicol Sci 107:404-415.

Groh K, Dalkvist T, Piccapietra F, Behra R, Suter M, Schirmer K. (2014). Critical influence of chloride ions on silver ion-mediated acute toxicity of silver nanoparticles to zebrafish embryos. Nanotoxicology 9:81-91.

Grossell M, Nielson C, Bianchini A. 2002. Sodium turnover rate determines sensitivity to acute copper and silver exposure in freshwater animals. Comp Biochem Physiol C 133:287-303.

He W, Zhou YT, Wamer WG, Boudreau MD, Yin JJ. 2012. Mechanisms of the pH dependent generation of hydroxyl radicals and oxygen induced by Ag nanoparticles. Biomaterials 33:7547-7555.

Howarth DL, Law SHW, Law JMcH, Mondon JA, Kullman SW, Hinton DE. 2012. Exposure to the synthetic FXR agonist GW4064 causes alterations in gene expression and sublethal hepatotoxicity in eleutheroembryo medaka (Oryzias latipes). Toxicol Appl Pharmacol 243: 111¯121.

Downloaded by [Duke University Libraries] at 13:10 30 June 2016

JUST ACCEPTED

Downloaded by [Duke University Libraries] at 13:10 30 June 2016

Hwang P-P, Lee T-H. 2007. New insights into fish ion regulation and mitochondrion-rich cells. Comp Biochem Physiol A 148:479-497.

Ivask A, Kurvet I, Karemets K, Blinova I, Aruoja V, Suppi S, Vija H, Kakinen A, Titma T, Heinlaan M, Visnapuu M, Koller D, Kisand V, Kahru A. 2014. Size-dependent toxicity of silver nanoparticles to bacteria, yeast, algae, crustaceans and mammalian cells in vitro. PLoS One 9: e102108.

Khan, F.R., Paul, K.B., Dybowska, A.D., Valsami-Jones, E., Lead, J.R., Stone, V. and Fernandes, T.F., 2015. Accumulation Dynamics and Acute Toxicity of Silver Nanoparticles to Daphnia magna and Lumbriculus variegatus: Implications for Metal Modeling Approaches. Environ Sci Technol 49:4389-4397.

Kim B, Park C-S, Murayama M, Hochella MF Jr. 2010. Discovery and characterization of silver sulfide nanoparticles in final sewage sludge products. Environ Sci Technol 44:7509-7514.

Kim TH, Kim M, Park HS, Shin US, Gong MS, Kim HW. 2012. Size-dependent cellular toxicity of silver nanoparticles. J Biomed Mater Res A, 100:1033-1043.

Kim K-T, Truong L, Wehmas L, Tanguay RL. 2013. Silver nanoparticle nanoparticle toxicity in the embryonic zebrafish is governed by particle dispersion and ionic environment. Nanotechnology 24:115101.

Kim S, Choi JE, Choi J, Chung K-H, Park K, Yi J, Ryu D-Y. 2009. Oxidative stress-dependent toxicity of nanoparticles in human hepatoma cells. Toxicol in Vitro 23:1076-1084.

JUST ACCEPTED

Downloaded by [Duke University Libraries] at 13:10 30 June 2016

Kwok KWH, Auffan M, Badireddy AR, Nelson CM, Wiesner MR, Chilkoti A, Liu J, Marinakos SM, Hinton DE. Uptake of silver nanoparticles and toxicity to early life stages of Japanese medaka (*Oryzias latipes*): effect of coating materials. Aquat Toxicol 120-121:59-66.

Laban G, Nies LF, Turco RF, Bickham JW, Sepulveda MS. 2010. The effects of silver nanoparticles on fathead minnow (*Pimephales promelas*) embryos. Ecotoxicol 19:185-195.

Lee B, Duong CN, Cho J, Lee J, Kim K, Seo Y, Kim P, Choi K, Yoon J. 2012. Toxicity of citrate-capped silver nanoparticles in common carp (*Cyprinus carpio*). J Biomed Biotechnol 2012:262670.

Ma R, Levard C, Marinakos SM, Cheng Y, Liu J, Michel FM, Brown GE Jr, Lowry GV. 2012. Size-Controlled Dissolution of Organic-Coated Silver Nanoparticles, Environ Sci Technol 46:752-759.

Massarsky A, Dupuis L, Taylor J, Eisa-Beygi S, Strek L, Trudeau VL, Moon TW. 2013. Assessment of nanosilver toxicity during zebrafish (*Danio rerio*) development. Chemosphere 92:59-66.

McCormick SD. 1995. Hormonal control of gill Na^+,K^+-ATPase and chloride cell function. In: Wood CM, Shuttleworth TJ, ed. Fish Physiology, Vol. 14, Cellular and Molecular Approaches to Fish Ionic Regulation. , New York: Academic Press, 285-315.

Pistilli M. 2011. Nanosilver market growth: Boon or bust for silver prices. Silver Investing News. Investing News Network®: Dig Media Inc.

The Project on Emerging Nanomaterials (2015). Washington, D.C.: Woodrow Wilson International Center for Scholars. http://www.nanotechproject.org. Accessed 30 Nov 2015.

JUST ACCEPTED

McShan D, Ray PC, Yu H. 2014. Molecular toxicity mechanism of nanosilver. J Food Drug Anal 22:116-127.

Navarro E, Piccapietra F, Wagner B, Marconi F, Kaegi R, Odzak N, Sigg L, Behra R. 2008. Toxicity of silver nanoparticles to *Chlamydomonas reinhardtii*. Environ Sci Technol 42:8959-8964.

Navarro E, Wagner B Odzak N, Sigg L, Behra R. 2015. Effects of Differently Coated Silver Nanoparticles on the Photosynthesis of *Chlamydomonas reinhardtii*. Environ Sci Technol 49: 8041-8047.

Nowack B. 2010. Nanosilver Revisited Downstream. Science 330:1054.

Park MVDZ, Neigh AM, Vermulen JP, de la Fonteyne LJJ, Verharen HW, Briede JJ, van Loveren H, de Jong WH. 2011. The effect of particle size on the cytotoxicity, inflammation, developmental toxicity and genotoxicity of silver nanoparticles. Biomaterials 32:9810-9817.

Peretyazhko TS, Zhang Q, Colvin VL. 2014. Size-controlled dissolution of silver nanoparticles at neutral and acidic pH conditions: kinetics and size changes. Environ Sci Technol 48:11954-11961.

Pham CH, Yi J, Gu MB. 2012. Biomarker gene response in male Medaka (*Oryzias latipes*) chronically exposed to silver nanoparticle. Ecotoxicol Environ Safe 78:239-245.

Rao X, Huang X, zhou Z, Lin X. 2013. An improvement of the 2^(-delta delta CT) method for quantitative real-time polymerase chain reaction data analysis. Biostat Bioinforma Biomath 3:71-85.

Downloaded by [Duke University Libraries] at 13:10 30 June 2016

JUST ACCEPTED

Downloaded by [Duke University Libraries] at 13:10 30 June 2016

Rasband, WS. 2015. ImageJ, US National Institutes of Health, Bethesda, MD, USA. http://imagej.nih.gov/ij/

Reidy B, Haase A, Luch A, Dawson KA, Lynch I. 2013. Mechanisms of Silver Nanoparticle Release, Transformation and Toxicity: A Critical Review of Current Knowledge and Recommendations for Future Studies and Applications. Materials 6:2295-2350.

Schultz AG, Ong KJ, MacCormack T, Ma G, Veinot JGC, Goss GG. 2012. Silver Nanoparticles Inhibit Sodium Uptake in Juvenile Rainbow Trout (Oncorhynchus mykiss). Environ Sci Technol 46:10295-10301.

Seltenrich N, 2013. Nanosilver: Weighing the Risks and Benefits. Environ Health Perspect 121:A220-A225.

Silver Nanotechnology Working Group, 2012. Nanosilver: Safety, Health and the Environmental Effects and Role of Antimicrobial Resistance. Comments of the Silver Nanotechnology Working Group for Review by the European Commission Scientific Committee on Emerging and Newly Identified Health Risks (SCENIHR). Durham, NC: Silver Nanotechnology Working Group, The Silver Research Consortium, LLC.

Suresh AK, Pelletier DA, Wang W, Morrell-Falvey JL, Gu B, Doktycz MJ. 2012. Cytotoxicity induced by engineered silver nanocrystallites is dependent on surface coatings and cell types. Langmuir 28:2727–2735.

Thermes V, Kin, C-C, Hwang, P-P 2010. Expression of Ol-foxi3 and Na^+/K^+ ATPase in ionocytes during the development of euryhaline medaka (*Oryzias latipes*) embryos. Gene Expr Patterns 10:185-192.

JUST ACCEPTED

Truong L, Tilton SC, Zaikova T, Richman E, Waters KM, Hutchison JE, Tanguay RL. 2013. Surface functionalities of gold nanoparticles impact embryonic gene expression responses. Nanotoxicology 7:192-201.

Van Aerle R, Lange A, Moorhouse A, Paszkiewicz K, Ball K, Johnston BD, de-Bastos E, Booth T, Tyler CR, Santos EM. 2013. Molecular mechanisms of toxicity of silver nanoparticles in zebrafish embryos. Environ Sci Technol 47:8005-8014.

Wang J, Wang W-X. 2013. Salinity influences on the uptake of silver nanoparticles and silver nitrate by marine medaka (*Oryzias melastigma*). Environ Toxicol Chem 33:632−640.

Wijnhoven SWP, Peijnenburg WJGM, Herberts CA, Hagens WI, Oomen AG, Heugens EHW, Roszek B, Bisschops J, Gosens, I, Ven de Meent D, Dekkers S, De Jong WH, van Zijverden M, Sips AJAM, Geertsma RE. 2009. Nano-silver – a review of available data and knowledge gaps in human and environmental risk assessment. Nanotoxicology 3: 109-138.

Wood CM, Hogstrand C, Galvez F, Munger RS. 1996. The physiology of waterborne silver toxicity in freshwater rainbow trout (*Oncorhynchus mykiss*): 2. The effects of silver thiosulphate. Aquat Toxicol 35:111-125.

Wood CM. 2011. Silver. In: Fish physiology: Homeostasis and toxicology of essential metals, Vol 31B. (eds: Wood CM, Farrell AP, Brauner CJ). Elsevier Publishers Sept 2013.

Wood CM, Marshall WS. 1994. Ion balance, acid-base regulation, and chloride cell function in the common killifish, *Fundulus heteroclitus*- a euryhaline estuarine teleosts. Estuaries 17:34-52.

Downloaded by [Duke University Libraries] at 13:10 30 June 2016

JUST ACCEPTED

Downloaded by [Duke University Libraries] at 13:10 30 June 2016

Wu S-C, Horng J-L, Liu S-T, Hwang P-P, Wen Z-H, Lin C-S, Lin L-Y. 2010. Ammonium-dependent sodium uptake in mitochondrion-rich cells of medaka (*Oryzias latipes*) larvae. Am J Physiol Cell Physiol C 298:237-250.

Wu M, Shariat-Madar B, Haron MH, Wu M, Khan IA, Dasmahapatra AK. 2011. Ethanol-induced attenuation of oxidative stress is unable to alter mRNA expression pattern of catalase, glutathione reductase, glutathione-S-transferase (GST1A), and superoxide dismutase (SOD3) enzymes in Japanese rice fish (*Oryzias latipes*) embryogenesis. Comp Biochem Physiol C 153:159-167.

Wu Y, Zhou Q 2013. Silver nanoparticles cause oxidative damage and histological changes in medaka (*Oryzias latipes*) after 14 days of exposure. Environ Toxicol Chem 32:165^{-1}72.

Yang X, Gondikas AP, Marinakos SM, Auffan M, Liu J, Hsu-Kim H, Meyer JN. 2012. Mechanism of silver nanoparticle toxicity is dependent on dissolved silver and surface coating in *Caenorhabditis elegans*. Environ Sci Technol 46:1119-1127.

Yin L, Cheng Y, Espinasse B, Colman BP, Auffan M, Wiesner M, Rose J, Liu J, Bernhardt ES. 2011. More than the ions: the effects of silver nanoparticles on *Lolium multiflorum. Environ Sci Technol 45:*2360-2367.

Yue Y, Behra R, Sigg L, Fernández Freire P, Pillai S, Schirmer K. 2014. Role of medium composition on silver nanoparticle toxicity to a fish gill cell line. Nanotoxicology 9:54-63.

Zhao CM, Wang WX. 2012. Importance of surface coatings and soluble silver in silverr nanoparticles toxicity to *Daphnia magna*. Nanotoxicol 6:361-370.

JUST ACCEPTED

Table 1. Properties of the silver nanoparticles (AgNPs) used in this study. Aggregate size, polydispersity index, zeta potential, and dissolved silver concentration at 24h and 96h after incubation. Dissolved silver concentrations are listed in units of μg l^{-1} (mean ± 1 sd) in suspensions of AgNPs with a total silver concentration of 10 mg Ag l^{-1}

Coating material		Polyvinylpyrrolidone				Gum arabic		Citrate	Citrate-Tannic acid		Citrate-Glutathione
Abbreviation		PVP				GA		Cit			
TEM diameter (nm)		49.6±8.5	38.2±9.9	8.4 ±2.3	7.1 ±3.3	5.5 ±2.7	22.83 ±6.0	7.2 ±10.9	24.4 ±5.1	39.1 ±9.1	25.9 ±9.1
Aggregate size (nm)	24h	109.9±10.3	97.6±8.4	122.3 ±7.4	107.2 ±11.6	96.2±16.5	80.9±18.1	38.5±9.7	186.4±12.1	136.2±184	263.6±104.3
	96h	95.4±8.1	89.5±6.8	101.3 ±19.8	102±12.1	849.0±151	1280.2±101	46.2±11.2	234.2±187	191.7±143	286.3±89.3
Polydispersity index	24h	0.298	0.244	0.351	0.357	0.358	0.377	0.555	0.455	0.790	0.641
	96h	0.236	0.226	0.246	0.355	0.491	0.507	0.566	0.542	0.892	1.000
Zeta potential (mV)	24h	-16.5±0.9	-14.2±0.6	-18.5±0.7	-14.3±1.2	-16.2 ±0.4	-20.8 ±0.4	-37.3±0.3	-26.1±1.2	-25.3±1.6	-19.5±1.5
	96h	-13. 3±1.4	-12.2±0.4	-14.3±0.6	-18.2±0.8	-16.5 ±6	-23.5±0.9	-26.2±0.6	-18.2±1.1	-27.9±1.8	-21.7±1.4
Dissolved Ag (μg l^{-1})	24h	92.5±2.4	26±2.1	159±3.4	127±4.0	146±3.5	15.7 ±2.3	143±3.4	187±5.1	7.0±1.3	91±2.7
	96h	81.5±3.4	25±1.9	138±2.5	196±3.7	133±5.6	30.3 ±1.2	100±2.4	199±6.2	10.9±1.5	106±3.1
Synthesis method and Characterization data reference		Coleman et al. 2014	Yang et al. 2012	Yang et al. 2012	Yang et al. 2012	Yin et al. 2011	Yin et al. 2011	Gondikas et al. 2009	Dadosh 2009	Dadosh 2009	Described in methods
TEM images reference		In supplementary information	Yang et al. 2012	Yang et al. 2012	Yang et al. 2012	Yin et al. 2011	Yin et al. 2011	Gondikas et al. 2009	In supplementary information	In supplementary information	In supplementary information

Downloaded by [Duke University Libraries] at 13:10 30 June 2016

JUST ACCEPTED

Table 2. Primer sequences used in this study.

Name	Primer sequence	Reference
MT		
forward	5’-CTCTTGCACCTGCACAAACTG-3’	Chae et al. 2009
reverse	5’-GCCAGATGCGCACTTAGTG-3’	
SOD		
forward	5’- GGCACTCTGTATGCCGGCTGC-3’	Pham et al. 2012
reverse	5’-GTTACCAAAGTCTCCCGGATG-3’	
CYP1a		
forward	5’-GGCCTACCCAGACATAGAAAAGAGA-3’	Wu et al. 2011
reverse	5’-AGTTGCTTCTGTCAGATATGGTAGGA-3’	
NKAa		
forward	5’GGAAGACAGCTACGGACAGC-3’	Wu et al. 2010
reverse	5’-GAGTTCCTCCTGGTCTTGCA-3’	
GST		
forward	5’-CACGGCCATCCTGAAATACCT-3’	Chae et al. 2009
reverse	5’-GTCAGCCGGGAACCAATGAT-3’	
18S RNA		
forward	5’-ATTGTCTGCCCTATCATCAACTTTC-3’	Howarth et al. 2010
reverse	5’-TGGATGTGGTAGCCGTTTC-3’	

Downloaded by [Duke University Libraries] at 13:10 30 June 2016

JUST ACCEPTED

Downloaded by [Duke University Libraries] at 13:10 30 June 2016

JUST ACCEPTED

Figure legends

Figure 1. 96h lethal concentration 50% (LC50) (mean ± sd) of ten silver nanoparticles of different coating materials and particle diameter (nm). Coating materials are indicated in the figure legend.

Figure 2. 96h lethal concentration 50% (LC50) (mean ± sd) of ten silver nanoparticles expressed in concentration of total dissolved silver in the test suspension. The horizontal line indicates the 96h LC50 value of silver nitrate for comparison.

Figure 3. Whole body total silver concentration (µg/g wet weight) of fish (mean ± sd) after silver nanoparticle exposure. Bars with different letters are statistically different.

Figure 4. Whole body total sodium concentration (µg/g wet weight) of fish (mean ± sd) after silver nanoparticle exposure expressed as percent relative to control. Bars with different letters are statistically different.

Figure 5. Whole body a) silver concentration and b) sodium concentration after exposure to ten silver nanoparticles vs. their respective 96h lethal concentration 50% values (mean ± 95%CI).

Figure 6. Representative sections and hyperspectral images of exposed fish: a) a dorsal-ventral section of medaka showing morphology of gill structures on either side of the midline (*arrow*), *L*, liver, *G*, gut, *A* atrium, *V*, ventricle, *Bc*, buccal cavity; b) hyperspectral image locating citrate 7nm silver nanoparticles (AgNPs) as red pixels in gills and the hyperspectral signal of the reference (white) and matching pixels (red) shown at the right bottom corner; c) enlarged image of area highlighted by the red box in panel b; d) a dorsal-ventral H&E stained section showing the fore- (*F*) and mid- (*M*) brain, *N*, opening nares with associated olfactory epithelium, *Ie*, inner ear; e) hyperspectral image locating PVP 38nm AgNPs as red pixels in the mid-brain.

Figure 7. Gene expression of fish (mean + sd) after exposure to ten silver nanoparticles and silver nitrate relative to control, a) glutathione sulfur transferase (GST), b) metallothionein (MT), c) superoxide dismutase (SOD), d) cytochrome P450 1a (CYP1a); and e) NA^{+}/K^{+} ATPase (NKA). Asterisks indicate statistical significant difference from control, * $p<0.05$, ** $p<0.01$, *** $p<0.001$.

Figure 8. Effect of silver nanoparticle (AgNP) exposure on expression of NA^{+}/K^{+} ATPase (NKA) gene and protein. Representative images of fish's right lateral abdominal surface showing expression of NKA gene (purple dots) and protein (brown dots) after exposure to a) clean water (control); the region of interest is indicated by red circle; b) gum arabic coated 6-nm AgNPs; c) citrate coated 7-nm AgNPs; d) polyvinylpyrrolidone (PVP) coated 7-nm AgNPs; e) an enlarged view of the right lateral abdominal surface to show NKA expressing cells; and f) the average number (error bar = sd) of cells expressing NKA gene (white bars) and protein (checked bars) per area on fish's right lateral abdominal surface. Asterisks indicate statistical significant difference from control, * $p<0.05$, ** $p<0.01$, *** $p<0.001$.

Figure 1

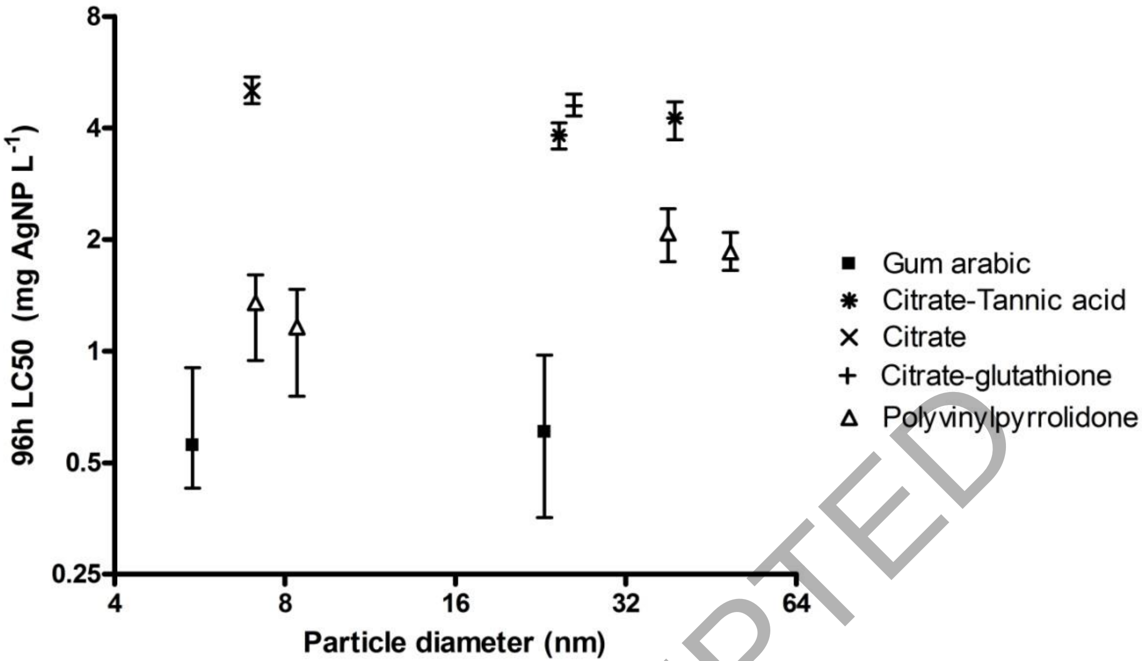

JUST ACCEPTED

Downloaded by [Duke University Libraries] at 13:10 30 June 2016

Figure 2

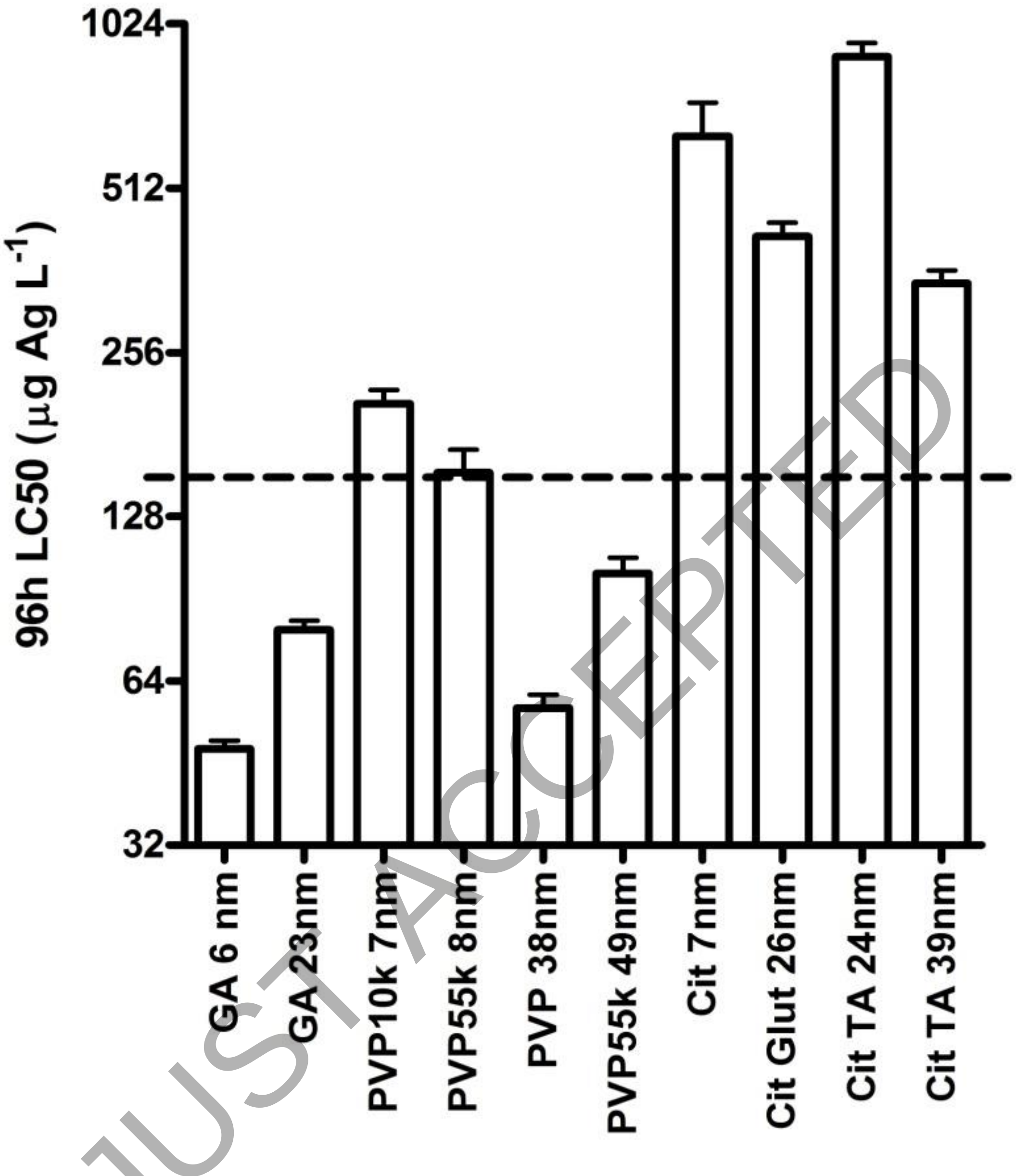

Downloaded by [Duke University Libraries] at 13:10 30 June 2016

JUST ACCEPTED

Figure 3

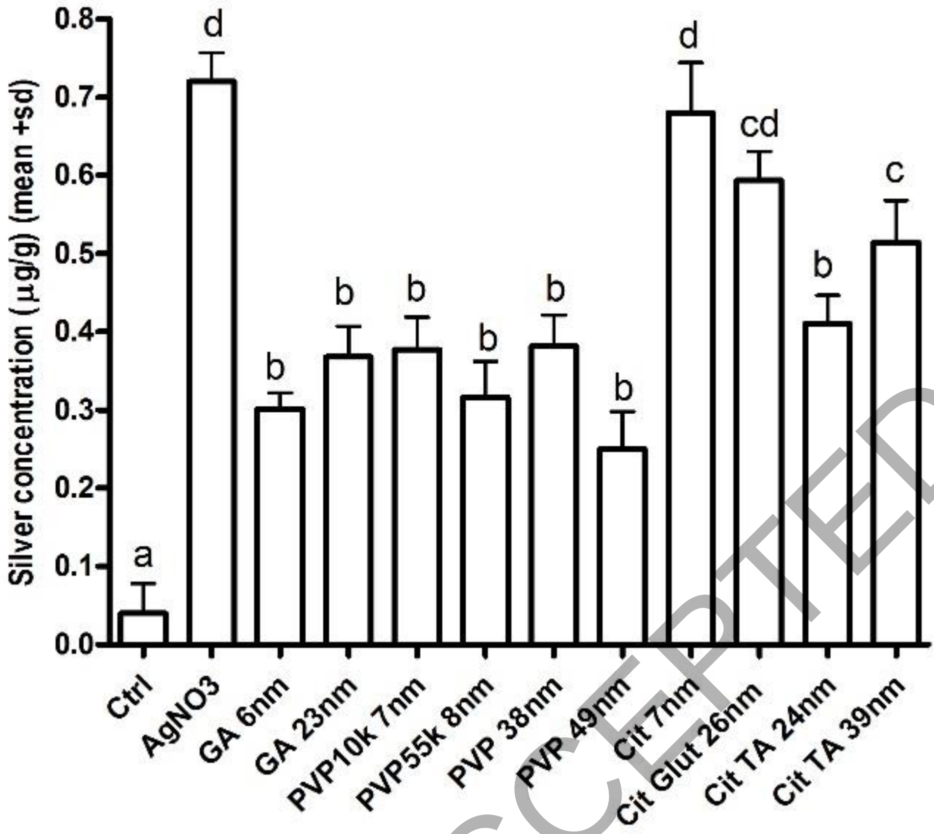

JUST ACCEPTED

Downloaded by [Duke University Libraries] at 13:10 30 June 2016

Fig 4

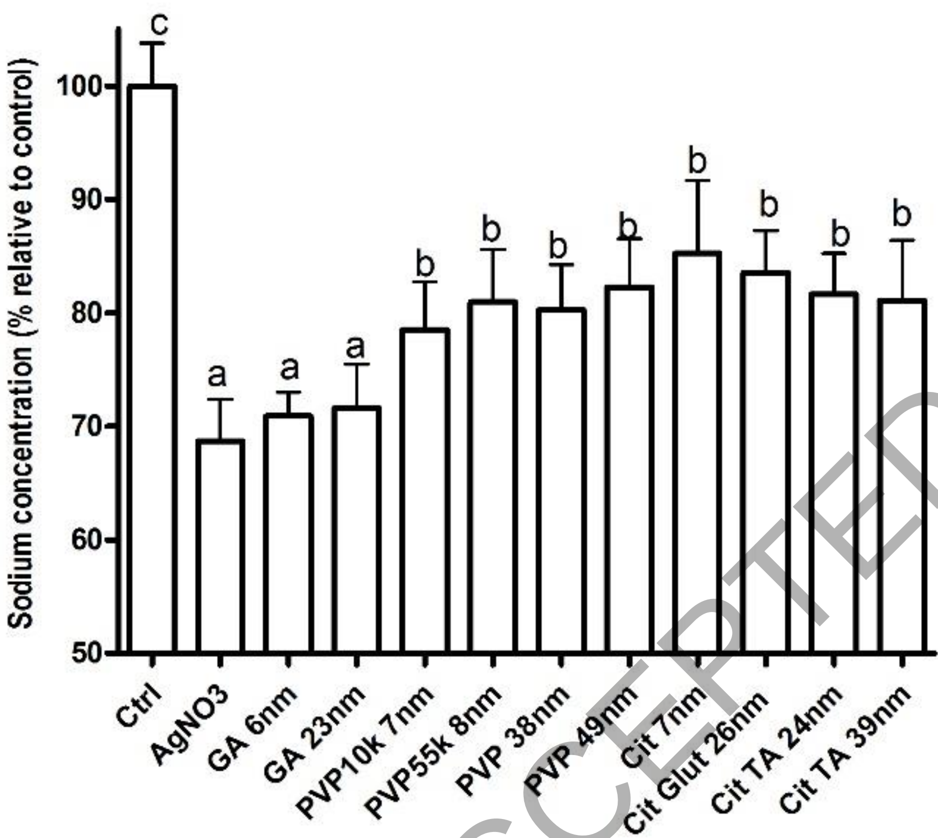

JUST ACCEPTED

Downloaded by [Duke University Libraries] at 13:10 30 June 2016

Fig 5

a

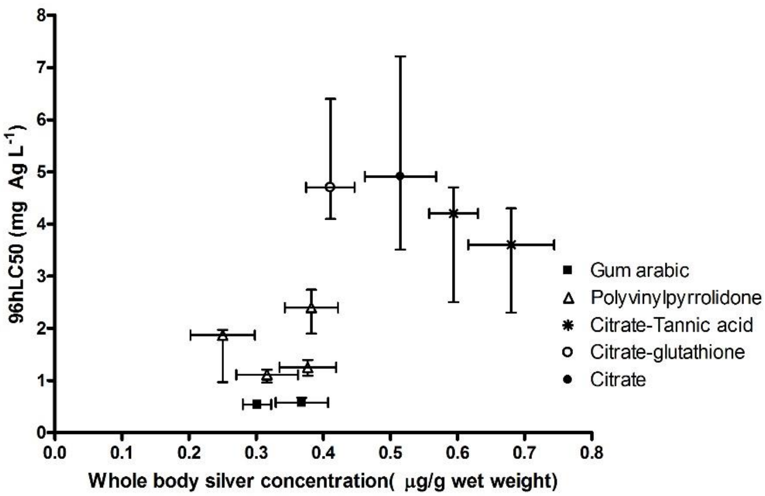

b

Downloaded by [Duke University Libraries] at 13:10 30 June 2016
JUST ACCEPTED

Fig. 6a

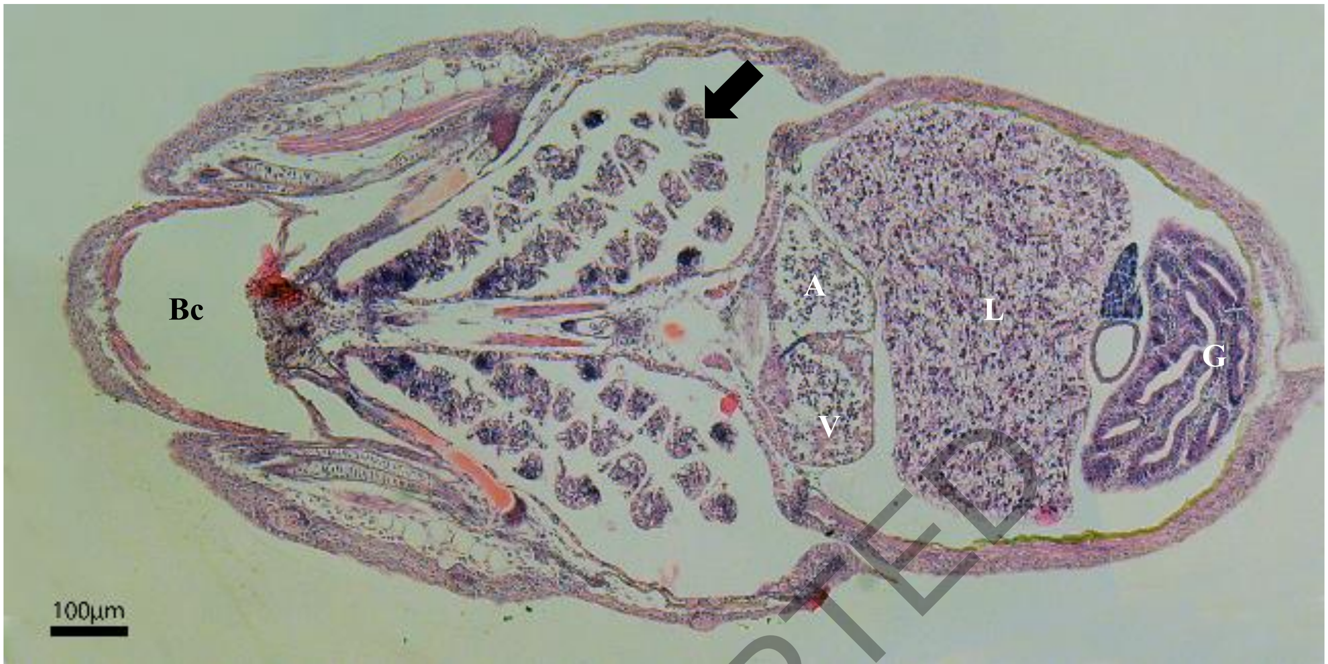

Downloaded by [Duke University Libraries] at 13:10 30 June 2016

JUST ACCEPTED

Fig. 6b

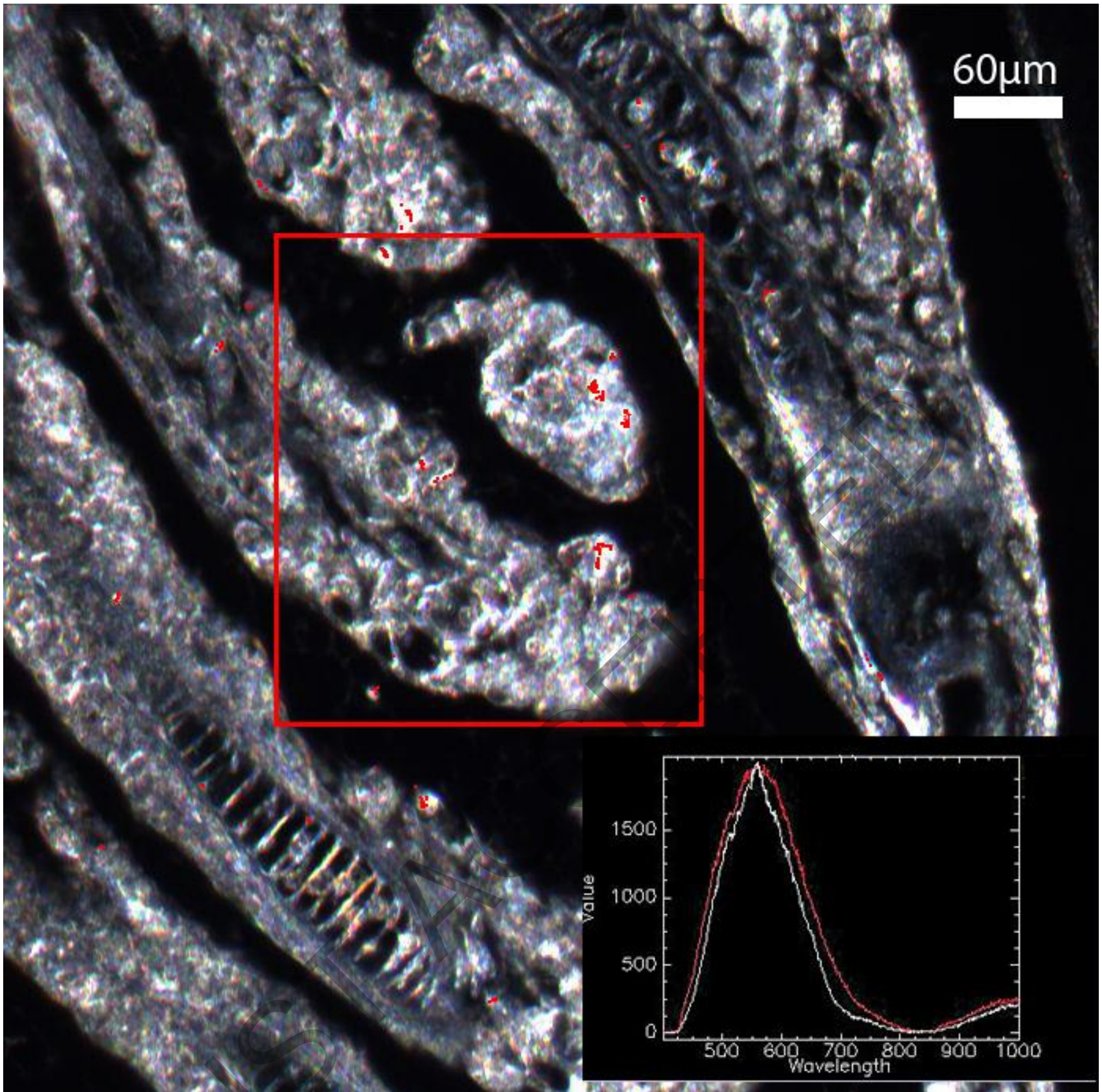

Downloaded by [Duke University Libraries] at 13:10 30 June 2016

JUST ACCEPTED

Fig. 6c

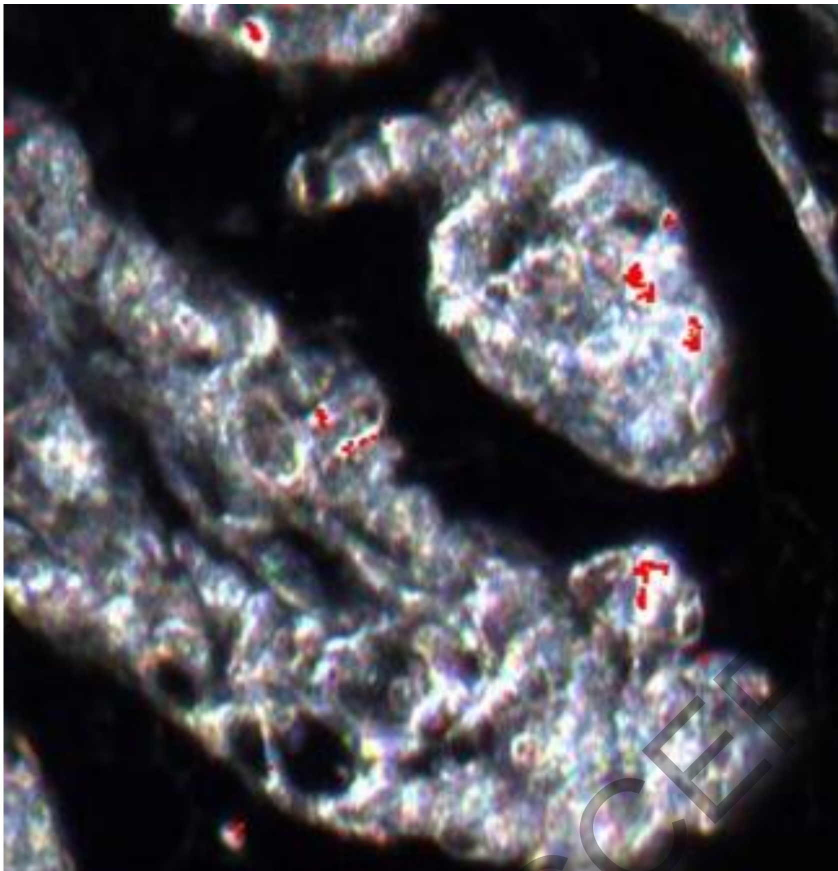

Downloaded by [Duke University Libraries] at 13:10 30 June 2016

JUST ACCEPTED

Fig. 6d

JUST ACCEPTED

Downloaded by [Duke University Libraries] at 13:10 30 June 2016

Downloaded by [Duke University Libraries] at 13:10 30 June 2016

Fig. 6e

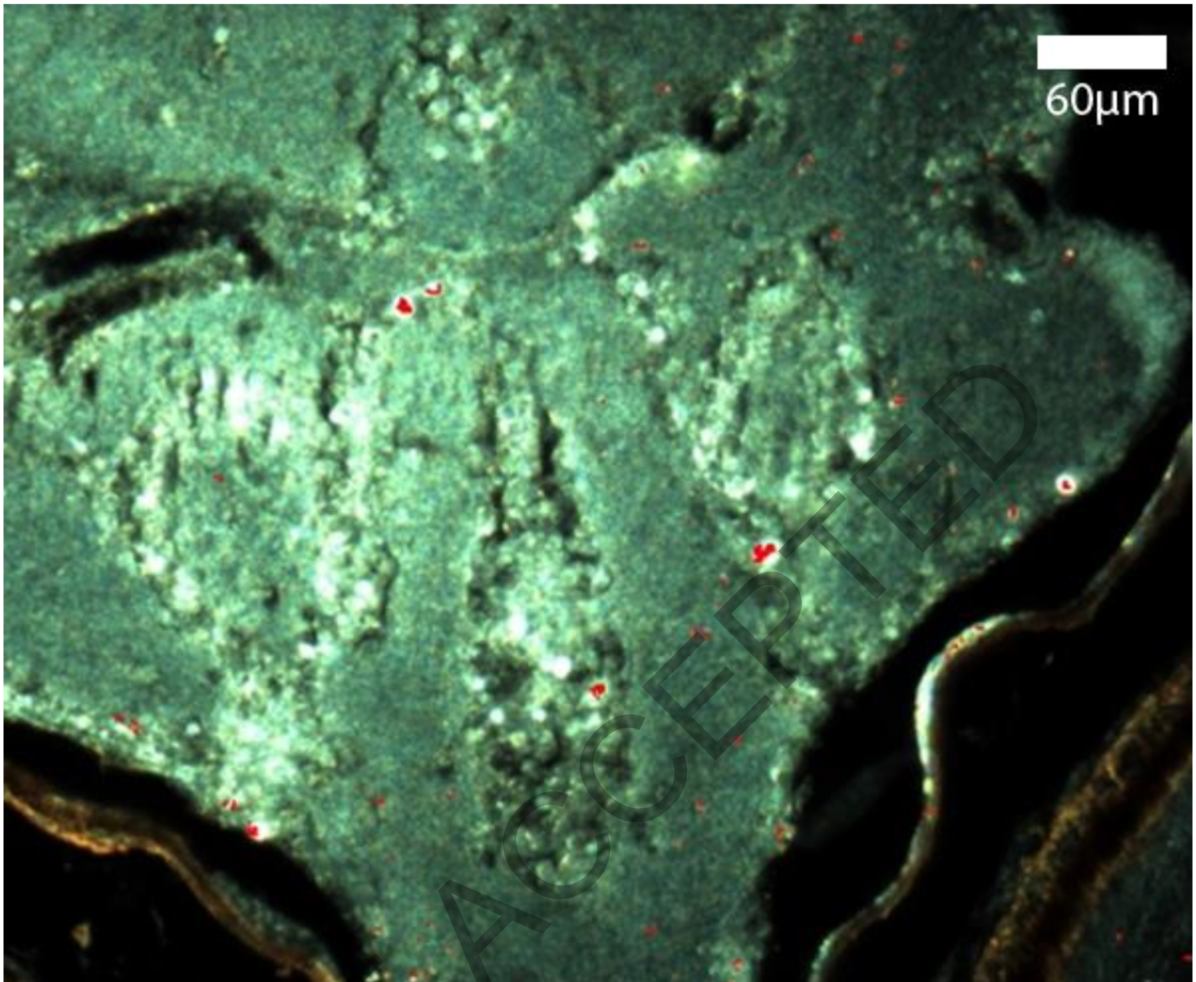

JUST ACCEPTED

Downloaded by [Duke University Libraries] at 13:10 30 June 2016

Fig. 7

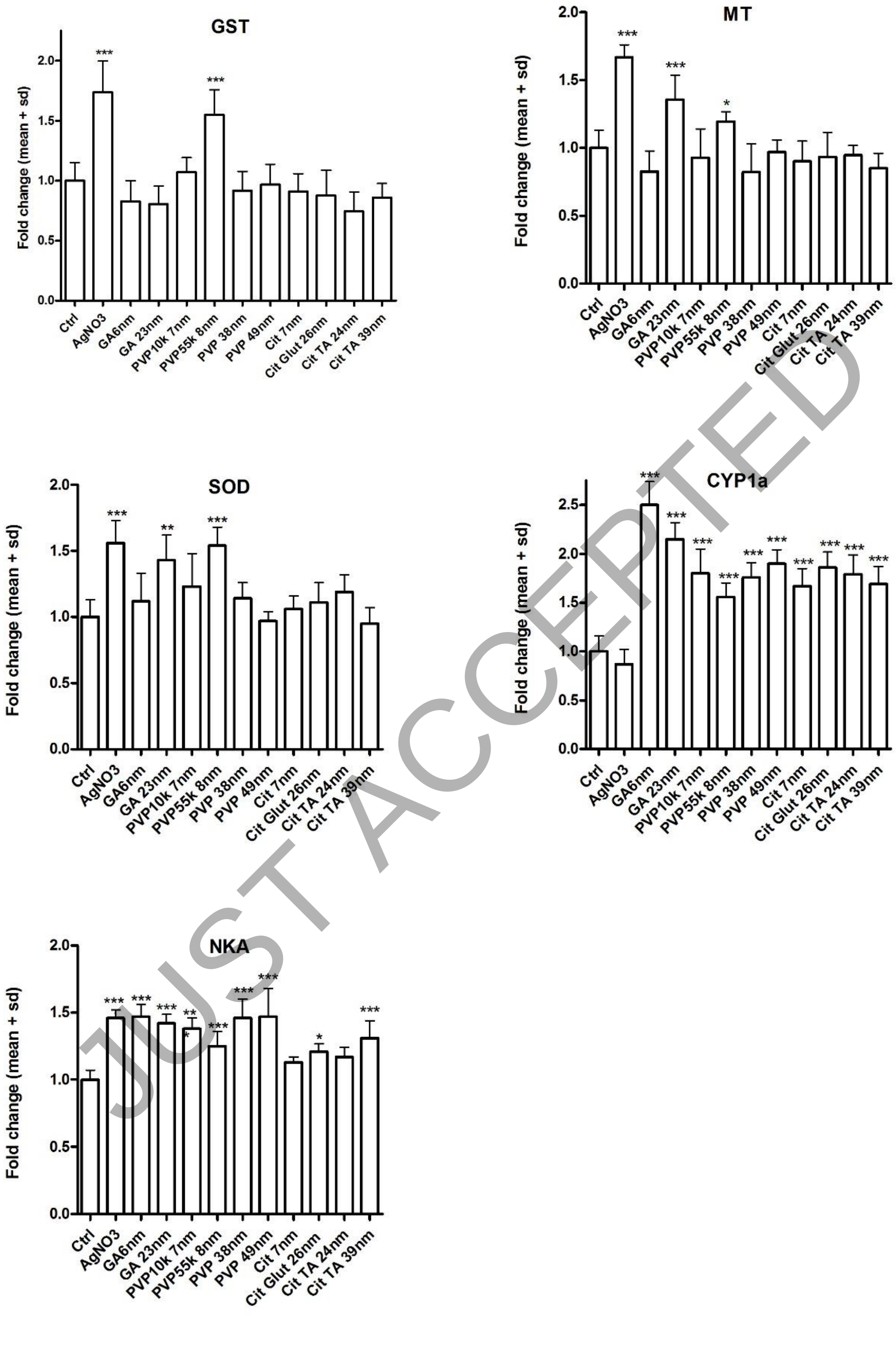

JUST ACCEPTED

Fig. 8

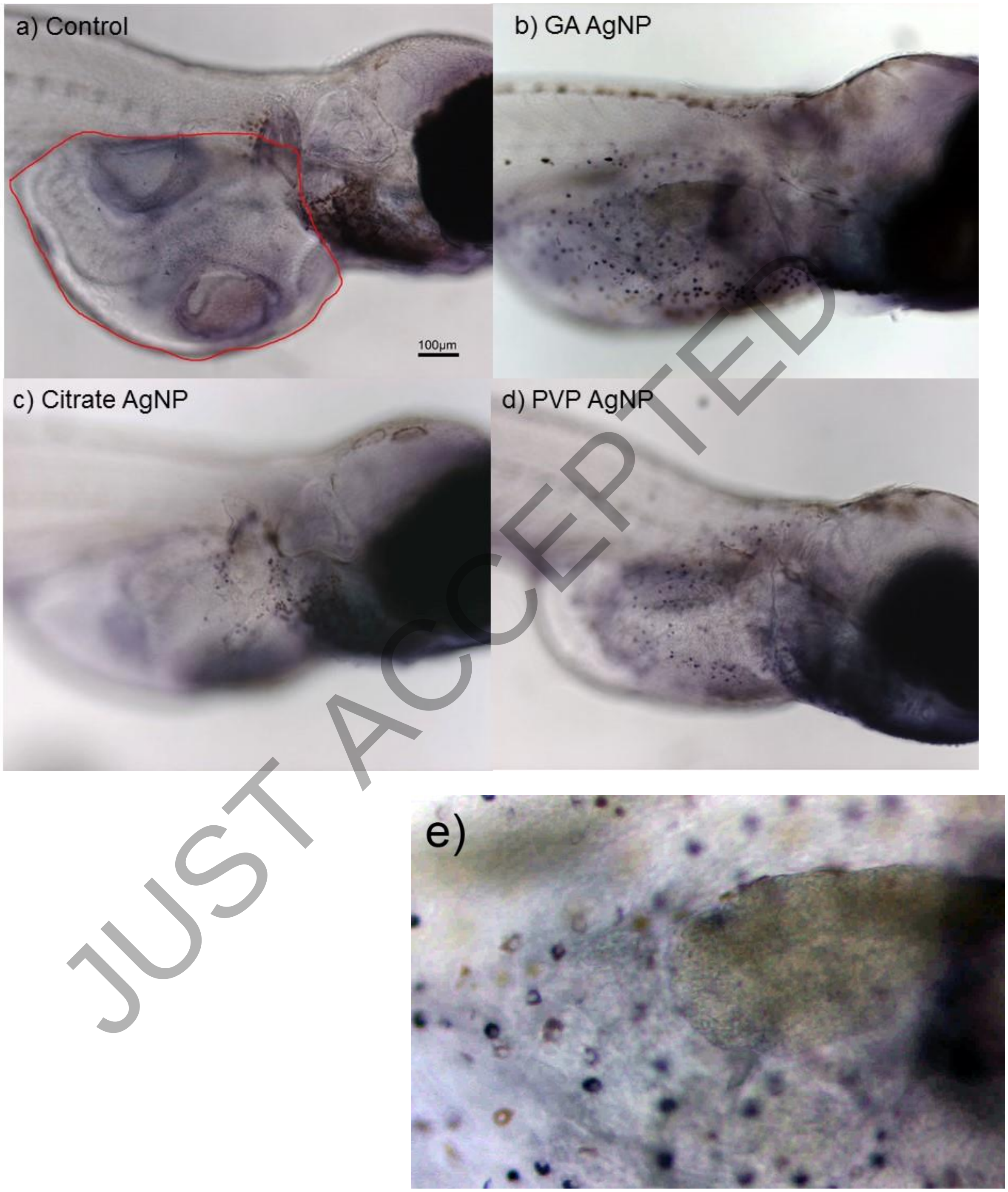

JUST ACCEPTED

Downloaded by [Duke University Libraries] at 13:10 30 June 2016

f)

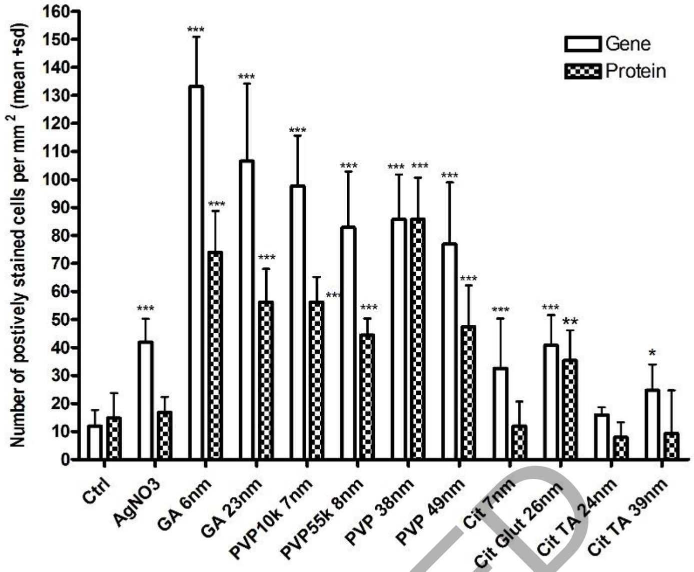

Downloaded by [Duke University Libraries] at 13:10 30 June 2016

JUST ACCEPTED